

A More Mechanistic Model of the Compression Strain–Load Response of Paper

T.J. URBANIK

A new strain–load relationship, including elastic strain and primary, secondary and tertiary phase components of creep strain, is proposed for paper: This new relationship unifies previous Forest Products Laboratory investigations in the creep of corrugated fibreboard and fibreboard containers. The rate-of-load effect on paper strain response and the chemical kinetics-based failure of materials. Physical constants in the relationship enable the continuous duration-of-load strain response of paper to be predicted from rate-of load stress–strain curves and vice versa.

Une nouvelle relation contrainte-charge, incluant la déformation élastique et les éléments des phases primaire, secondaire et tertiaire de la déformation due au fluage, est proposée pour le papier. Cette nouvelle relation permet l'unification des essais des anciens Laboratoires des produits forestiers effectués sur les cartonnages ordinaires et ondulés, l'effet du taux de charge sur la réponse du papier à la contrainte, et la défaillance attribuable à la cinétique chimique des matériaux. Les constantes physiques de la relation permettent de prévoir la réponse pendant toute la durée de la charge de contrainte sur le papier à partir des courbes contrainte-déformation et inversement.

INTRODUCTION

The time-dependent deformation of paper and corrugated fibreboard under stress is well recognized as an indicator of eventual material rupture and product service life. Researchers have sought various models for predicting the collapse or otherwise rupture of specimens following the primary and secondary phases of creep of specimens enduring a constant load, i.e. duration-of-load (DOL) tests. The primary creep phase is an initial rapid straining of material following the theoretically instantaneous load application; the secondary creep phase is the subsequently longer phase during which the creep rate eventually stabilizes or at least slows toward a minimum. A tertiary phase with another rapid increase in straining precedes ultimate specimen rupture.

Moody and Skidmore [1] observed that the secondary creep in DOL compression tests of corrugated boxes stabilizes at a constant rate. Koning and Stem [2] quantified the relationship between this secondary creep rate and stacking life of corrugated boxes, and at least

four other subsequent researchers [3-6] corroborated these findings. As summarized by Bronkhorst [6], the collective significance of the secondary creep rate should make this parameter a target for greater understanding.

Improved data acquisition techniques enabled Urbanik [7] to characterize continuous DOL creep and creep rate variations with time for corrugated fibreboard under edgewise compression and cyclic relative humidity (RH). Specimen strain was observed to creep at a rate in accordance with a first-order mathematical system, and to vary from a rate initiating primary creep to an eventual steady state and lower rate that characterized the secondary creep phase. The rate of change was quantifiable by a system time constant. Kuskowski [5] later utilized the same first-order model for corrugated tubes. By contrast, tension researchers [8,9] proposed DOL creep characterizations for paper strips wherein the secondary creep rate decreases with each decade of time. The focus of this paper is on the compression response of paper for its application to corrugated containers.

An alternative model introduced by Caulfield [10] is to substitute a rate-of-load (ROL) test - i.e. load increasing linearly with time until failure - for a DOL test. The relationship between the applied load and the time to fail in a DOL test was formulated in terms of constants that also relate failure load to loading

rate in an ROL test [10]. Thus, DOL performance can predict ROL performance and vice versa. ROL tests are less time consuming than their DOL partners and seemingly more favourable. However, to date, load-deformation data have not been found to readily yield a quantifiable creep rate as obtainable from DOL tests.

Although it makes some sense to conclude the relationship between ROL strength and DOL time-to-failure on the basis of the model [10] alone, a more mechanistic understanding of ROL phenomena is obtainable from the shape of the strain–load curve preceding failure and the values of physical constants believed to relate to the secondary creep rate. To this end, the work reported here reexamines some ROL data from Gunderson et al. [11] on the compression response of paper. The objective is a more mechanistic model of the compression strain–load curve for obtaining a load-dependent secondary creep rate. Few new assumptions beyond those already implemented by former paper investigators are introduced, so the model presented here further unifies the status of compression creep research.

CREEP THEORY - CONSTANT LOAD

A review of some previous DOL research sets forth the equations from which we

JPPS

T.J. Urbanik
Forest Products Lab.
USDA Forest Service
One Gifford Pinchot Drive
Madison, WI, USA
53705-2398
(urbanik@fs.fed.us)

TABLE I
CREEP STRAIN AND STRAIN RATE EXPRESSIONS FOR PASES 1, 2 AND 3

| Phase | Strain rate $\dot{\epsilon}_{ci}$ | Creep strain $\dot{\epsilon}_{ci}$ (constant p) | Creep strain $\dot{\epsilon}_{ci}$ ($p = rt$) |
|-------|-----------------------------------|---|--|
| 1 | $(R_1 - R_2)e^{-t/t_1}$ | $t_1(R_2 - R_1)(e^{-t/t_1} - 1)$ | $R_1 = q_0(1 - a_1) + a_1 R_2, R_2 = q_0 e^{q_1 p}, R_3 = b_0 + b_1 R_2$ $\frac{t_1(1 - a_1)q_0}{1 - t_1 q_1 r} (e^{q_1 r t} e^{-t/t_1} - 1) - t_1(1 - a_1)q_0(e^{-t/t_1} - 1)$ |
| 2 | R_2 | $R_2 t$ | $\frac{q_0}{q_1 r} (e^{q_1 r t} - 1)$ |
| 3 | $R_3 e^{-t/t_3}$ | $t_3 R_3 (e^{-t/t_3} - 1)$ | $\int_0^t (b_0 + b_1 q_0 e^{q_1 r t}) e^{-a e^{-b r t} / t_3} e^{-t/t_3} dt$ |

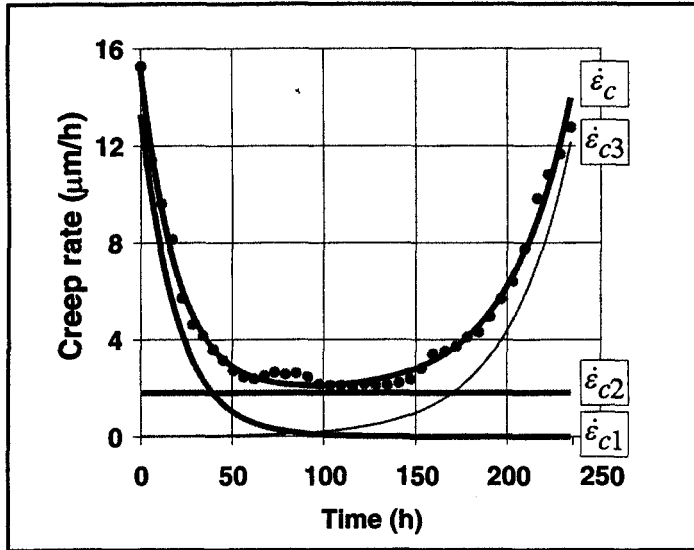


Fig. 1. Fit of Eq. (5) to DOL data on creep rate variation with time of a 38 mm column specimen of corrugated fibreboard subjected to 1.75 kN/m static edgewise compression and 50 to 90% cyclic RH [7]. $R_1 = 15.1 \mu\text{m/h}$, $R_2 = 1.81 \mu\text{m/h}$, $R_3 = 12.2 \mu\text{m/h}$, $t_1 = 19.7 \text{ h}$, $t_3 = 33.6 \text{ h}$ and $t_b = 234 \text{ h}$.

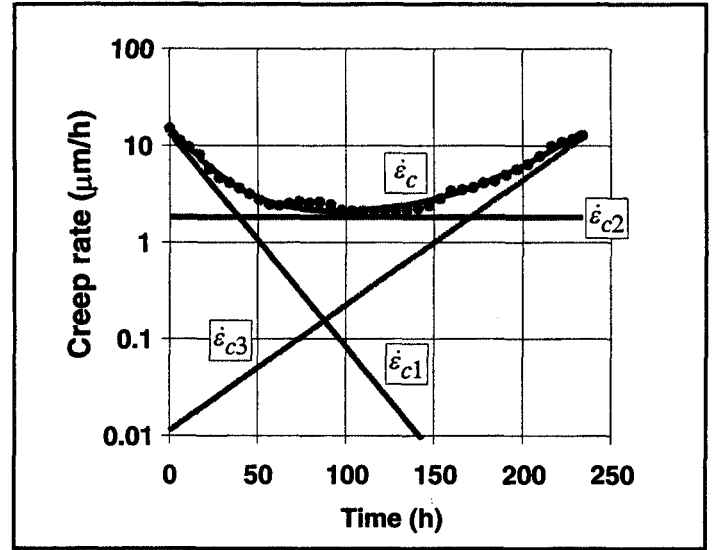


Fig. 2. DOL data from Fig. 1 scaled to show linear decrease in $\log \dot{\epsilon}_{c1}$ with time and simultaneous linear increase in logs, 3. Slopes of in $\dot{\epsilon}_{c1}$ and $\ln \dot{\epsilon}_{c3}$ are $-1/t_1$ and $1/t_3$, respectively.

derive the physical constants to be introduced later in our ROL theory. Monkman and Grant [12] found an empirical relationship between rupture life and secondary creep rate of metal alloys. Koning and Stem [2] applied this relationship to corrugated fibreboard boxes subjected to constant compression, relating the time t_b to failure with the secondary creep rate R_2 observed during the earliest determinable portion of secondary creep, using the formula

$$t_b = A \frac{1}{R_2^x} \quad \text{or} \quad \ln t_b = \ln A - x \ln R_2 \quad (1)$$

where A and x are empirical constants. Unique evaluations of A and x in Eq. (1) were determined to be applicable to a composite of stacking height, container content, relative humidity, load level and various fabrication variables. Paper researchers [13] observed the same relationship for paper under edgewise compression and cyclic humidity, but in contrast with corrugated fibreboard, A and x depended on the material.

For more general materials, Caulfield [10] related t_b to the constant load p in a DOL test with the formula

$$p = \frac{1}{b} \ln a - \frac{1}{b} \ln t_b \quad \text{or} \quad t_b = a e^{-bp} \quad (2)$$

Although constants a and b appear simply as empirical, they represent the derived combination of more fundamental variables characterizing molecular motion in accordance with a theory of chemical kinetics. Equating t_b from Eqs. (1) and (2) predicts that R_2 should vary with p according to

$$R_2 = q_0 e^{q_1 p} \quad \text{or} \quad \ln R_2 = \ln q_0 + q_1 p \quad (3)$$

where

$$q_0 = \left(\frac{A}{a}\right)^{1/x} \quad \text{and} \quad q_1 = \frac{b}{x} \quad (4)$$

are creep-rate-load constants.

As mentioned previously, continuous characterizations of creep strain E , and creep strain rate $\dot{\epsilon}_c = dE/dt$ were determined [7] from the sum of phase components

$$\dot{\epsilon}_c = \dot{\epsilon}_{c1} + \dot{\epsilon}_{c2} + \dot{\epsilon}_{c3} \quad (5)$$

Expressions for $\dot{\epsilon}_{c1}$, $\dot{\epsilon}_{c2}$ and $\dot{\epsilon}_{c3}$ during primary, secondary and tertiary phases of creep, respectively, at constant p are given in the second column of Table I. In our previous work [7], only the first two creep phases were considered, but

now the third phase is also accounted for. Creep rate R_1 is the initial rate of the sum of $\dot{\epsilon}_{c1}$ and $\dot{\epsilon}_{c2}$ at $t = 0$, and R_3 is the terminal rate of $\dot{\epsilon}_{c3}$ at $t = t_b$. Time constants t_1 and t_3 characterize the rate of creep rate change during the first and third phases, respectively. A fit of Eq. (5) to the DOL data [7] is shown in Fig. 1. The contribution of each phase to total creep rate is more readily discernible from Fig. 2, which shows how $\log \dot{\epsilon}_{c1}$ decreases linearly with time at a rate $-1/t_1$, while $\log \dot{\epsilon}_{c3}$ increases linearly with time at a rate $1/t_3$.

Expressions for creep strain ϵ_c characterizing each creep phase can be determined from integrating each component of Eq. (5):

$$\epsilon_c = \epsilon_{c1} + \epsilon_{c2} + \epsilon_{c3} \\ = \int_0^t \dot{\epsilon}_{c1} dt + \int_0^t \dot{\epsilon}_{c2} dt + \int_0^t \dot{\epsilon}_{c3} dt \quad (6)$$

Results at constant p are given in the third column of Table I and are compared with data in Fig. 3.

CREEP THEORY - RATE OF LOAD

If, instead of being fixed, load is applied

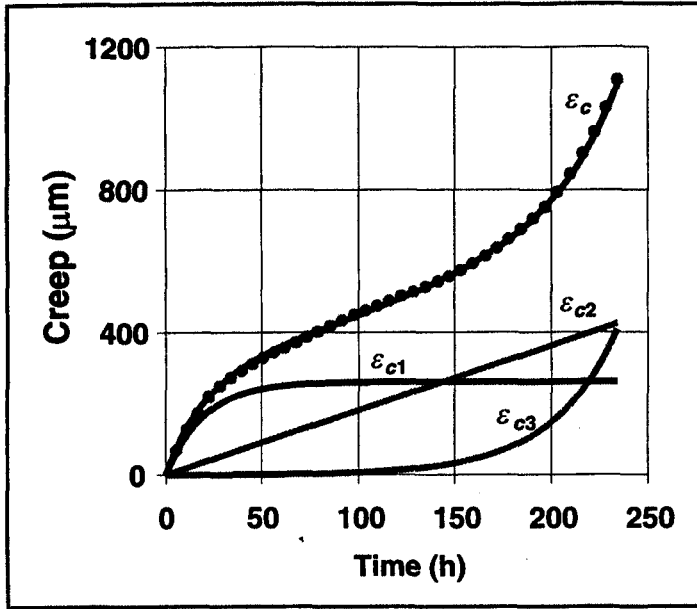


Fig. 3. Plot of Eq. (6) compared with DOL data on creep deformation variation with time obtained from same specimen in Fig. 1. Physical parameter values are the same as those in Fig. 1.

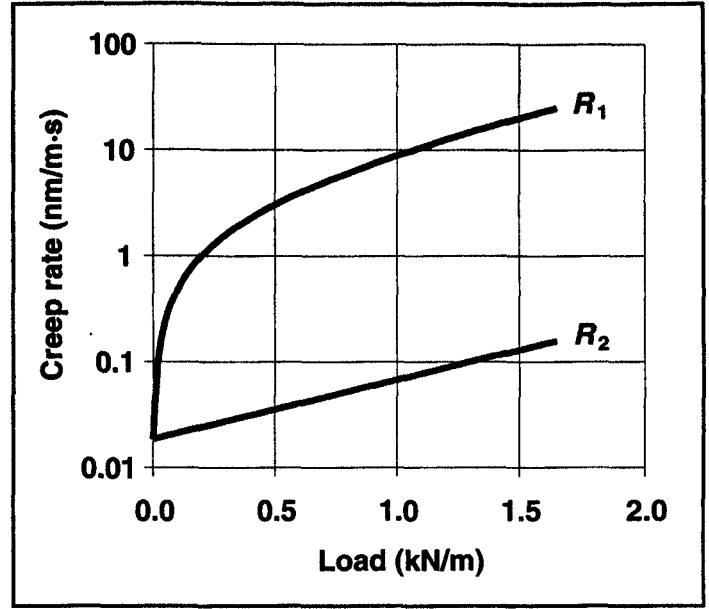


Fig. 4. Plots of R_2 according to Eq. (3) and R_1 according to Eq. (10). Material properties are those of experimental design B-CD-50 from Table I.

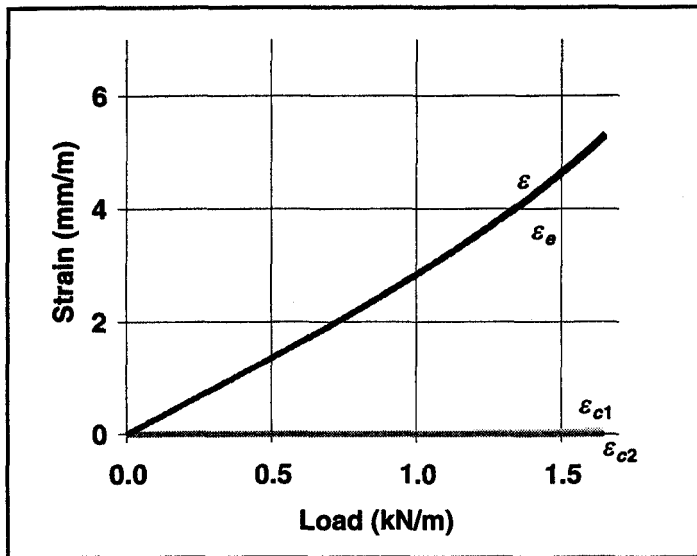


Fig. 5. Plots of component terms in the equation $e = e_e + e_{c1} + e_{c2}$, with material properties representing experimental design B-CD-50 and with loading rate $r = 263 \text{ N/m-s}$. Maximum load occurs at $t = 6.3 \text{ s}$. In such a rapid test, e is essentially indiscernible from e_e , and e_{c1} is indiscernible from e_{c2} .

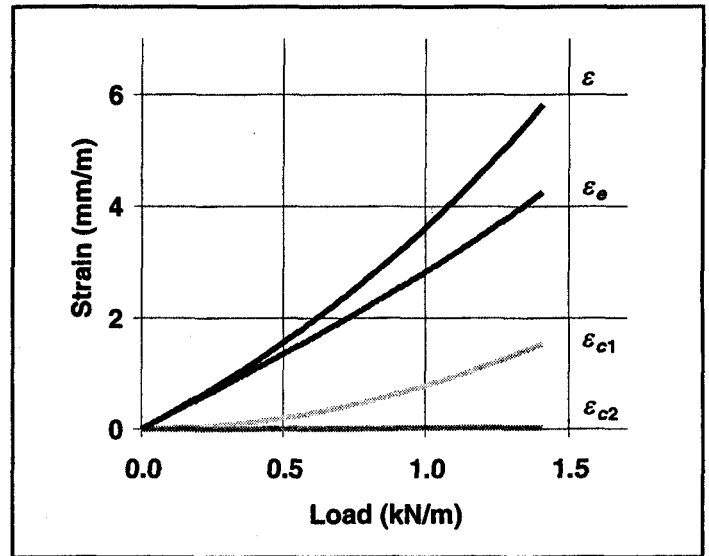


Fig. 6. Plots of component terms in the equation $e = e_e + e_{c1} + e_{c2}$, with material properties representing experimental design B-CD-50 and with loading rate $r = 2.63 \text{ N/m-s}$. Maximum load occurs at $t = 8.9 \text{ min}$ compared to $t_i = 8.1 \text{ min}$; creep is in accordance with a primary creep mechanism.

linearly with time at a rate r such that

$$p = rt \quad (7)$$

then total strain e is the sum of an elastic strain e_e depending only on stress and the irreversible e_c depending on stress and time. With the edgewise compression of paper, data on the variation of p with e_e [14] have been found to fit the formula

$$p = c_1 \tanh\left(\frac{c_2}{c_1} \epsilon_e\right) \quad (8)$$

where c_1 and c_2 are empirical constants.

Equation (8) was applied to a study of

the effect of r on the edgewise compression response of paper [11]. Researchers conducted ROL tests spanning five decades of r . They substituted e for e_e in Eq. (8) and examined how fitted constants c_1 and c_2 depended on r . Stiffness was considered to be merely the initial slope of the load-strain curve without separately accounting for e_c . Values of c_2 , the initial slope of Eq. (8), increased with increasing r and by the definition of stiffness in [11] led to an apparent stiffening of the load-strain curve as load rate increased.

A more accurate rate-independent definition of stiffness is given by the slope of Eq. (8). If strain is measured in response to a vary-

ing applied load, the inverse of Eq. (8) given by

$$\epsilon_e = \frac{c_1}{2c_2} \ln\left(\frac{c_1 + p}{c_1 - p}\right) \quad p < c_1 \quad (9)$$

is a more appropriate formula to fit to data. To introduce e_c via Eq. (6) into an ROL expression for E , the integration must account for variation in R_1 , R_2 , R_3 and t_b (Table I) with p as t increases. Few investigations are known that quantify how R_1 and R_3 for paper might depend on other variables. From ROL experiments to be discussed in subsequent sections of this paper, we can now infer that

$$R_1 = q_0(1 - \alpha_1) + \alpha_1 R_2 \quad (10)$$

and follows a variation with p as predicted by Eq. (3) (Fig. 4). Substituting Eqs. (2), (7) and (10) into Eq. (6) thus leads to the implicitly p -dependent expressions for ϵ_{c1} and ϵ_{c2} as given in the fourth column of Table I. An expression proposed for ϵ_{c3} based on the linear relationship

$$R_3 = \beta_0 + \beta_1 R_2 \quad (11)$$

is also given, but as noted ϵ_{c3} needs to be determined numerically.

Values of a and b appearing in the expression for ϵ_{c3} (Table I) can be determined from ROL failure data. Caulfield's [10] companion formula to Eq. (2) proposes that the ROL failure load P varies with r according to

$$P = \frac{1}{b} \ln ab + \frac{1}{b} \ln r \quad (12)$$

which yields a and b from a collection of strain-load curves up to failure. With a and b thus determined, the ROL strain relationship

$$\epsilon = \epsilon_e + \epsilon_{c1} + \epsilon_{c2} + \epsilon_{c3} \quad (13)$$

has components in terms of Eqs. (6) and (9) and is predicted to be a function of the physical constants $c_1, c_2, q_0, q_1, a_1, t_1, b_0, b_1$ and t_3 .

Some features of Eq. (13), including primary and secondary creep phases, are shown in Figs. 5–7, where E is plotted as the sum of its elastic and creep components at each of three loading rates. Material constants representing experimental design B–CD–50 from Table II in the next section were chosen. The plot of ϵ_e is the same in each figure except for the maximum load corresponding to failure at each loading rate.

If the loading rate is high enough and failure occurs at a time much less than t_1 for the material, almost no creep occurs, and the difference between E and E_e is essentially indiscernible (Fig. 5). At a lower loading rate such that the testing time is on the order of t_1 (Fig. 6), creep follows a primary creep mechanism corresponding to what would occur during the early phase of DOL creep. As the loading rate is further lowered and testing time exceeds t_1 (Fig. 7), primary creep dissipates and creep occurs according to a secondary creep mechanism. Collectively these plots (Figs. 5–7) illustrate the importance in differentiating between primary and secondary creep mechanisms when comparing DOL and ROL data

COMPARISON WITH DATA

Data from former ROL research [11] were analyzed to establish representative parameter values in our model. The researchers had examined a 205 g/m² linerboard (A) and a 127 g/m² corrugating medium (B) in the machine direction (MD) and cross-machine direction (CD) at two levels of RH, 50 and 90%. Strain-load curves with six specimen replications per test combination were generated until failure at load rates of 263, 2.63 and 0.0263 N/m-s. These researchers determined a composite fit for each set of six replicated curves at each of the three load rates. Our new model en-

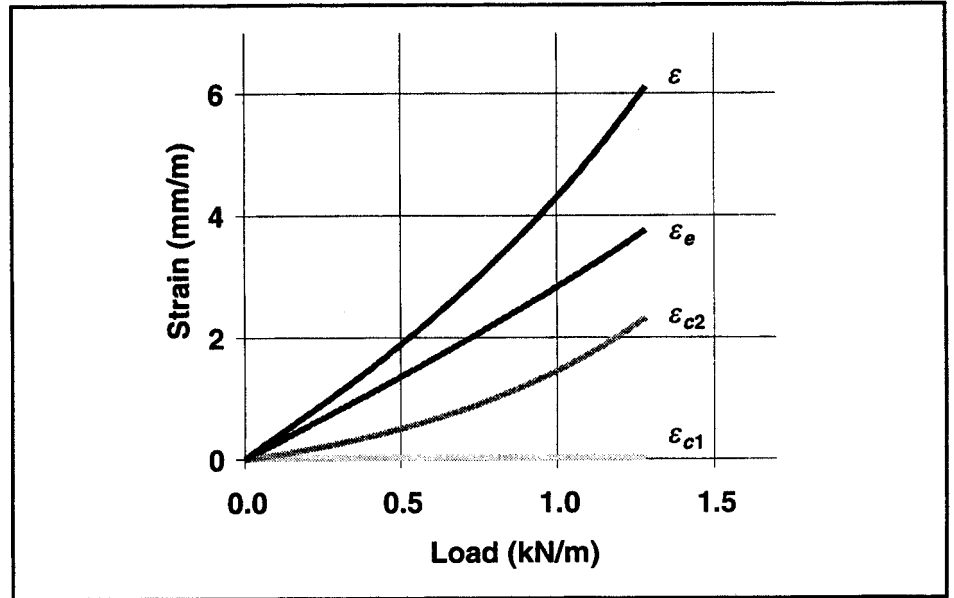


Fig. 7. Plots of component terms in the equation $\epsilon = \epsilon_e + \epsilon_{c1} + \epsilon_{c2}$, with material properties representing experimental design B–CD–50 and with loading rate $r = 0.0263$ N/m-s. Maximum load occurs at $t = 13.5$ h compared to $t_1 = 0.13$ h. In contrast with Fig. 6, creep is in accordance with a secondary creep mechanism.

| Experimental design | | | Strain-load analysis | | | | | |
|---------------------|-----------|--------|----------------------|--------------|----------------|--------------|---------|-------|
| Material | Direction | RH (%) | c_1 (kN/m) | c_2 (kN/m) | q_0 (nm/m-s) | q_1 (mm/N) | t (s) | a_1 |
| A | MD | 50 | 8.23 | 2217 | 1.54 | 0.484 | 6766 | 24 |
| | | 90 | 4.58 | 1699 | 6.87 | 0.728 | 714 | 172 |
| | CD | 50 | 4.81 | 1022 | 2.15 | 1.05 | 553 | 285 |
| B | MD | 50 | 2.75 | 690 | 13.6 | 1.19 | 668 | 196 |
| | | 90 | 5.49 | 1140 | 3.21 | 1.12 | 3540 | 19 |
| | CD | 50 | 1.91 | 749 | 26.7 | 1.26 | 342 | 178 |
| | | 90 | 2.52 | 374 | 18.6 | 1.30 | 485 | 180 |
| | | 90 | 1.22 | 264 | 31.8 | 3.52 | 321 | 87 |

RH: relative humidity; MD: machine direction; CD: cross-machine direction

| Experimental design | | | Average P (kN/m) at three r levels | | | Failure constants | |
|---------------------|-----------|--------|--|--------------|----------------|-------------------|------------|
| Material | Direction | RH (%) | 263 (N/m-s) | 2.63 (N/m-s) | 0.0263 (N/m-s) | $\ln a$ (ln s) | b (mm/N) |
| A | MD | 50 | 5.30 | 5.02 | 4.45 | 56.9 | 10.8 |
| | | 90 | 3.65 | 2.84 | 2.41 | 26.0 | 7.43 |
| | CD | 50 | 3.64 | 3.03 | 2.90 | 43.1 | 12.5 |
| B | MD | 50 | 2.40 | 1.85 | 1.67 | 28.3 | 12.6 |
| | | 90 | 3.29 | 2.88 | 2.31 | 30.3 | 9.40 |
| | CD | 50 | 1.67 | 1.26 | 1.05 | 23.0 | 14.9 |
| | | 90 | 1.65 | 1.41 | 1.28 | 38.7 | 24.9 |
| | | 90 | 1.05 | 0.86 | 0.73 | 27.9 | 28.8 |

abled us to fit a composite to all 18 curves. Strength data to which we also fit Eq. (12) are summarized in Table III along with the $\ln a$ and b evaluations.

A series of fits of Eq. (13) to data were made to refine our model based on the minimization of prediction errors and the statistical confidence intervals of model parameters. The first series yielded consistently large values for t_3 from which a simpler model for tertiary creep was inferred from the limiting case as t_3 approaches infinity:

$$\lim_{t_3 \rightarrow \infty} \epsilon_{c3} = b_0 t + b_1 \epsilon_{c2} \quad (14)$$

The next series of fits with ϵ_{c3} defined either by Eq. (14) or by its subset forms (i.e. $b_0 = 0$ and $b_1 = 0$) were not found to quantify tertiary creep with any statistical significance. As c_1 increases, the term $b_0 t$ approaches the form of ϵ_e , and as t_1 decreases, the term $b_1 \epsilon_{c2}$ approaches the form of ϵ_{c2} , making Eq. (14) statistically confounded with expressions for ϵ_e and ϵ_{c2} . An independent tertiary creep mechanism derived from Eq. (11) is not

discernible from Gunderson's data [11]. The fact that each specimen within a group of six replicates failed at a different load makes the quantification of tertiary creep based on average failure in a group difficult and warrants a different experimental design for quantifying ROL tertiary creep.

With Eq. (13) truncated to include only primary and secondary creep mechanisms, the model $\epsilon = \epsilon_e + \epsilon_{c1} + \epsilon_{c2}$ was fit to the data and was tested with various forms of the linear relationship $R_1 = \mathbf{a}_0 + \mathbf{a}_1 R_2$. Neglecting \mathbf{a}_0 , the simple proportionality of $R_1 = \mathbf{a}_1 R_2$ was first tried, but this predicted an E offset at the lowest r , which was inconsistent with data. The magnitude of offset was found to be equal to the limiting case as r becomes infinitesimally small.

$$\lim_{r \rightarrow 0} \epsilon_{c1} \Big|_{d_0=0} = \tau_1 (1 - \alpha_1) q_0 (e^{-t/\tau_1} - 1) \quad (15)$$

This led to the value of $\mathbf{a}_0 = q_0 (1 - \alpha_1)$ which, when incorporated into the integration of $\dot{\epsilon}_{c1}$, yields a correction term equal to Eq. (15) and a more accurate prediction of ϵ_{c1} at all r levels.

Final results of our composite fits are given in Table II, along with precision estimates by an approximated standard error associated with each parameter value in Table IV. Two experimental designs, A-CD-50 and B-CD-50, yielded consistently high precision (low standard errors) for all material properties. Among the other experimental designs, estimates of q_0 and q_1 appear to be the least sensitive. A trial was made to prescribe q_0 and q_1 as a function of A and x in accordance with Eq. (4) and then determine the optimum values of A and x representing all material sets. However, the resulting fits deviated too far from data to be considered useful, and the results as given in Table II are more accurate.

Although our composite values of c_1 and c_2 in Table II are overall highly correlated with the composite values reported in Gunderson et al. [11], with correlation coefficients of 0.995 and 0.998 for c_1 and c_2 , respectively, differences between the two studies were observed in the effect of RH on these constants. At 50% RH, our composite values of c_1 are on average 18% greater than those reported by Gunderson, and at 90% RH the difference is 6.5%. At 50% RH, our composite values of c_2 are on average 3% lower than those of Gunderson, and at 90% RH they are 7.4% greater.

PREDICTIONS AT CONSTANT LOAD

Expressions for the components of Eq. (13) at a constant p are given in the third column of Table I. Figure 8 shows creep strain plots of Eq. (13) based on material properties from experimental design B-CD-50, if instantaneous loads of $0.1P$, $0.35P$, $0.6P$, $0.75P$ and $0.8P$ were applied. P is the ROL strength at 263 N/m.s. Over the time scale shown, the curves at $0.75P$ and $0.8P$ are truncated at a time of failure predicted by Eq. (2). Although there are no data for verifying these curves (Fig. 8), the predicted curves for paper in Fig. 8 have the same form as the experimental data during primary and secondary creep of corrugated fibreboard (Fig. 3).

| Experimental design | | | Standard error (%) | | | | | | |
|---------------------|-----------|--------|--------------------|-------|------------------|------------------|-----|-------|--|
| Material | Direction | RH (%) | c_1 | c_2 | q_0 | q_1 | t | a_1 | |
| A | MD | 50 | 3 | 0 | 24 | >10 ⁴ | 0 | 84 | |
| | | 90 | 2 | 1 | 8 | >10 ⁴ | 0 | 16 | |
| | CD | 50 | 3 | 1 | 16 | 8 | 17 | 21 | |
| | | 90 | 3 | 0 | >10 ⁴ | >10 ⁴ | 0 | 6 | |
| B | MD | 50 | 4 | 0 | 16 | >10 ⁴ | 0 | 49 | |
| | | 90 | 7 | 0 | >10 ⁴ | 3 | 21 | 17 | |
| | CD | 50 | 3 | 1 | 6 | 6 | 20 | 14 | |
| | | 90 | 10 | 0 | >10 ⁴ | 0 | 20 | 13 | |

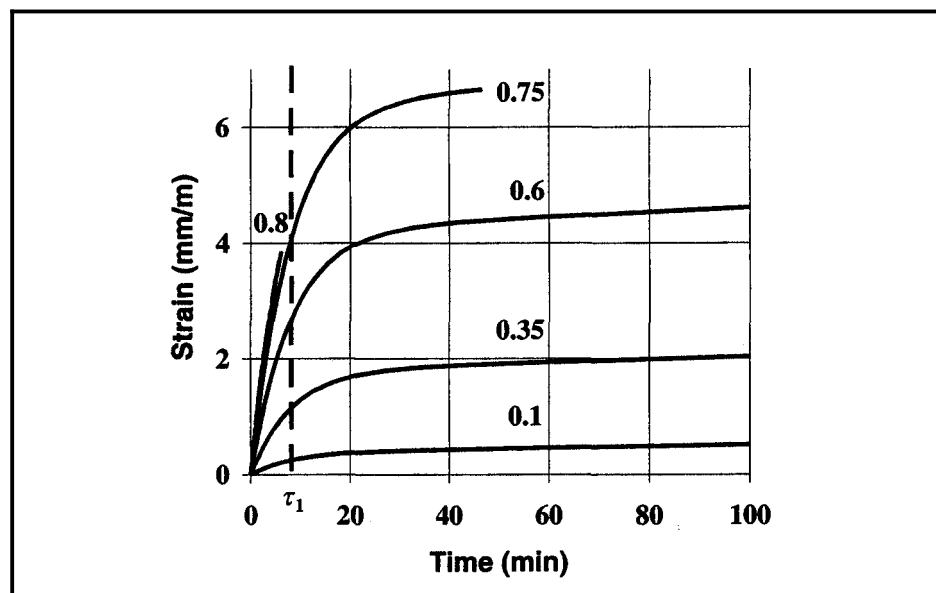


Fig. 8. Plots of Eq. (13) representing predicted DOL creep response at load levels corresponding to $0.1P$, $0.35P$, $0.6P$, $0.75P$ and $0.8P$ where P is ROL material strength at 263 N/m.s and Eq. (13) inputs are based on material properties from experimental design B-CD-50.

COMMENTS AND CONCLUSIONS

A new stress-strain relationship including elastic and irreversible creep strain components is proposed for paper. Expressions for creep rate characterizing constant load data are integrated to determine corresponding expressions for creep strain. To further generalize these creep strain expressions and deal with a linearly increasing load, our model incorporates the relationships among load level, creep rate and failure time from other previous Forest Products Laboratory investigations, thereby unifying these studies. The results enable DOL and ROL data to be characterized in terms of the same physical constants. Fits of our model to data were determined from previous ROL experiments on containerboard materials. Such tests successfully characterized the primary and secondary phases of creep, but new and different experiments appear to be warranted to better quantify tertiary creep.

In actual service, the containerboard components of corrugated containers are subjected to neither a constant duration of load nor a linearly increasing load. Changes in humidity and moisture content within various components would impose cyclical stresses upon an average load. Since our expressions for

strain in response to a linearly increasing load were derived by integrating appropriate expressions between an initial zero time and a terminal time, the analysis can be broadened easily to integration between arbitrary time limits representing an infinitesimal time increment. Such results would provide a way to represent any load profile with a numerical summation of linear load segments and to examine the strain response to humidity-induced loads. In addition, our model can also be used to determine a zero-to-failure loading profile that spans multiple load rates and enables all the physical constants in the model to be determined from a single stress-strain curve.

REFERENCES

1. MOODY, R.C. and SKIDMORE, K.E., "How Dead Load, Downward Creep Influence Corrugated Box Design", *Package Eng.* August (1966).
2. KONING, J.W., Jr. and STERN, R.K., "Long-Term Creep in Corrugated fibreboard Containers", *Tappi* 60(12):128-131 (1977).
3. LEAKE, C.H., "Measuring Corrugated Box Performance", *Tappi J.* 71(10):71-75 (1988).
4. LEAKE, C.H. and WOJCIK, R., "Influence of the

- Combining Adhesive on Box Performance", *Tappi J.* 72(8):61-65 (1989).
5. KUSKOWSKI, S.J., LEE, S.K. and VERRILL, S.P., "Hygroexpansivity - Papermaking Variables and Corrugated Container Stacking Behavior", Project 368-1, Phase 3, for Containerboard and Kraft Paper Group, AF&PA (1995).
 6. BRONKHORST, C.A., "Toward a More Mechanistic Understanding of Corrugated Container Creep Deformation Behaviour", *J. Pulp Paper Sci.* 23(4):J174-J181 (1997).
 7. URBANIK, T.J., "Hygroexpansion-Creep Model for Corrugated Fibreboard", *Wood and Fiber* 27(2):134-140 (1995).
 8. BREZINSKI, J.P., "Creep Properties of Paper", *Tappi J.* 39(2):116-128 (1956).
 9. HASLACH, J.W., JR., PECHT, M.G. and WU, X., "Variable Humidity and Load Interaction in Tensile Creep of Paper, Proc. Intl. Paper Physics Conf., TAPPI PRESS, 219-224 (1991).
 10. CAULFIELD, D.F., "A Chemical Kinetics Approach to the Duration-of-Load Problem in Wood", *Wood Fibre Sci.* 17(4):504-521 (1985).
 11. GUNDERSON, D.E., CONSIDINE, J.M. and SCOTT, C.T., "The Compressive Load-Strain Curve of Paperboard: Rate of Load and Humidity Effects", *J. Pulp Paper Sci.* 14(2):J37-J41 (1988).
 12. MONKMAN, F.C. and GRANT, N.J., "An Empirical Relationship Between Rupture Life and Minimum Creep Rate in Creep-Rupture Tests", *Proc. ASTM* 56:593-621 (1956).
 13. CONSIDINE, J.M., GUNDERSON, D.E., THELIN, P. and FELLERS, C., "Compressive Creep Behavior of Paperboard in a Cyclic Humidity Environment - Exploratory Experiment", *Tappi J.* 72(11):131-136 (1989).
 14. URBANIK, T.J., "Method Analyzes Analogue Plots of Paperboard Stress-Strain Data", *Tappi J.* 65(4):104-108 (1982).

REFERENCE: URBANIK, T.J., A More Mechanistic Model of the Compression Strain-Load Response of Paper, 28(6):211-216 June 2002. Paper offered as a contribution of the Journal of Pulp and Paper Science. Not to be reproduced without permission from the Pulp and Paper Technical Association of Canada. Manuscript received August 29, 2000; rev ised manuscript aproved for publication by the Review Panel November 28, 2001.

KEYWORDS: PAPER, STRESS STRAIN PROPERTIES, CREEP, MATHEMATICAL MODELS.